

# AN ADVANCED BEAM ELEMENT FOR THE ANALYSIS OF STEEL STRUCTURES

**Evangelos J. Sapountzakis**

Professor

School of Civil Engineering, National Technical University of Athens  
Zografou Campus, GR-157 80, Athens, Greece

e-mail: [cvsapoun@central.ntua.gr](mailto:cvsapoun@central.ntua.gr)

**Ioannis C. Dikaros**

Civil Engineer, MSc, PhD Student

School of Civil Engineering, National Technical University of Athens  
Zografou Campus, GR-157 80, Athens, Greece

e-mail: [dikarosciannis@gmail.com](mailto:dikarosciannis@gmail.com)

## 1. ABSTRACT

In this paper an “advanced” 20x20 stiffness matrix and the corresponding nodal load vector of a beam element of arbitrary composite cross taking into account shear lag effects due to both flexure and torsion is applied for the analysis of steel framed structures. Nonuniform warping distributions, which are responsible for shear lag effects are taken into account by employing four additional degrees of freedom.

## 2. INTRODUCTION

In engineering practice the analysis of spatial frames is frequently encountered. The involved beam members of such structures are usually analyzed employing Euler-Bernoulli or Timoshenko beam theories. Both theories maintain the assumption that cross sections remain plane after deformation. Thus, the formulation remains simple; however it fails to capture “shear lag” phenomenon which is associated with a significant modification of normal stress distribution due to nonuniform shear warping [1,2]. In up-to-date regulations, the significance of shear lag effect in flexure is recognized. However in order to simplify the analysis, the “effective breadth” concept is recommended. This simplifying approach may fail to capture satisfactorily the actual structural behavior of the member. Therefore, it is necessary to include nonuniform shear warping effects in the analysis. Similar considerations with the ones made for flexure could be also adopted for the problem of torsion which is also very often encountered in the analysis of spatial frames (e.g. in curved-in-plan bridges, buildings of complex geometry etc.). It is well-known, that a beam under general twisting loading and boundary conditions, is led to nonuniform torsion. The major characteristic of this problem is the presence of normal stress due to primary torsional warping. In an analogy with Timoshenko beam theory when shear deformation is important, Secondary Torsional Shear Deformation Effect (STSDE) [3,4] has to be taken

into account as well. The additional secondary torsional warping due to STSDE causes similar effects with shear lag in flexure, i.e. a modification of the initial normal stress distribution.

In the present study, an advanced 20x20 stiffness matrix and the corresponding nodal load vector of a member of arbitrary cross section taking into account shear lag effects due to both flexure and torsion, is constructed. Nonuniform warping distributions, which are responsible for shear lag effects are taken into account by employing four independent warping parameters, multiplying a shear warping function in each direction [1] and two torsional warping functions, which are obtained by solving corresponding boundary value problems. Ten boundary value problems with respect to kinematical components are formulated and solved using the Analog Equation Method [5], a BEM based technique. The warping functions and the geometric constants including the additional ones due to warping are evaluated employing a pure BEM approach. The aforementioned problems are formulated employing an improved stress field arising from the correction of shear stress components.

### 3. STATEMENT OF THE PROBLEM

Consider a prismatic element of length  $l$  with an arbitrarily shaped composite cross section consisting of materials in contact, each of which can surround a finite number of inclusions, with modulus of elasticity  $E_m$  and shear modulus  $G_m$ , occupying the regions  $\Omega_m$  ( $m=1,2,\dots,M$ ) of the  $yz$  plane (Fig.1). The materials of these regions are assumed homogeneous, isotropic and linearly elastic.  $CXYZ$  is the principal bending coordinate system through centroid  $C$ , while  $y_C, z_C$  are its coordinates with respect to  $Sxyz$  system through shear center  $S$ . The beam element is subjected to arbitrarily distributed or concentrated axial loading  $p_x(X)$ , transverse loading  $p_y(x), p_z(x)$ , twisting moment  $m_x(x)$ , bending moments  $m_Y(x), m_Z(x)$  and to warping moments (bimoments)  $m_{\phi_x^p}(x), m_{\phi_y^p}(x), m_{\phi_z^p}(x), m_{\phi_x^s}(x)$  (Fig.1) [1].

Under the action of the aforementioned loading and of possible restraints, the beam member is led to nonuniform flexure and/or nonuniform torsion. It is well-known that the bending moment at a cross section represents the distribution of normal stresses due to bending (**primary normal stresses**  $\sigma_{xx}^p$ ). Due to variation of this moment along the beam, shear stresses arise on the cross sectional plane which, contrary to Timoshenko theory exhibit a nonuniform distribution. These shear stresses will be referred to as **primary** (or St.Venant) **shear stresses** ( $\tau_{xy}^p, \tau_{xz}^p$ ) and lead the cross section to warp (Fig.2b). Due to the nonuniform character of this warping along the beam **secondary normal stresses**  $\sigma_{xx}^s$  are developed (Fig.2c). These normal stresses are responsible for shear lag phenomenon and they are taken into account by employing an independent warping parameter multiplying a warping function, depending on the cross sectional configuration. The nonuniform distribution of secondary normal stresses  $\sigma_{xx}^s$  along the beam results is equilibrated by **secondary shear stresses**  $\tau_{xy}^s, \tau_{xz}^s$  (Fig.2d). However, from Fig.3d it can be concluded in analogy to Timoshenko theory that  $\tau_{xy}^s, \tau_{xz}^s$  arising from the use of the independent warping parameter fail to fulfill the boundary condition related to vanishing tractions  $\tau_{xn}$  on the lateral surface of the beam. Thus, in the present study a modified stress field is applied

with the aid of an additional warping function in order to “correct”  $\tau_{xy}^S, \tau_{xz}^S$  (Fig.3e). The above remarks are also valid for the problem of nonuniform torsion taking into account secondary torsional shear deformation effect – STSDE [3,4]. In order to take into account torsional shear lag effects as well, the normal stress distribution  $\sigma_{xx}^S$  due to secondary torsional warping  $\varphi_x^S$  [4] is also taken into account. This distribution is equilibrated by corresponding tertiary shear stresses  $\tau_{xz}^T, \tau_{xy}^T$  which, similarly with the case of shear lag analysis in flexure, require a correction. In the present study this is achieved by adding an additional torsional warping function.

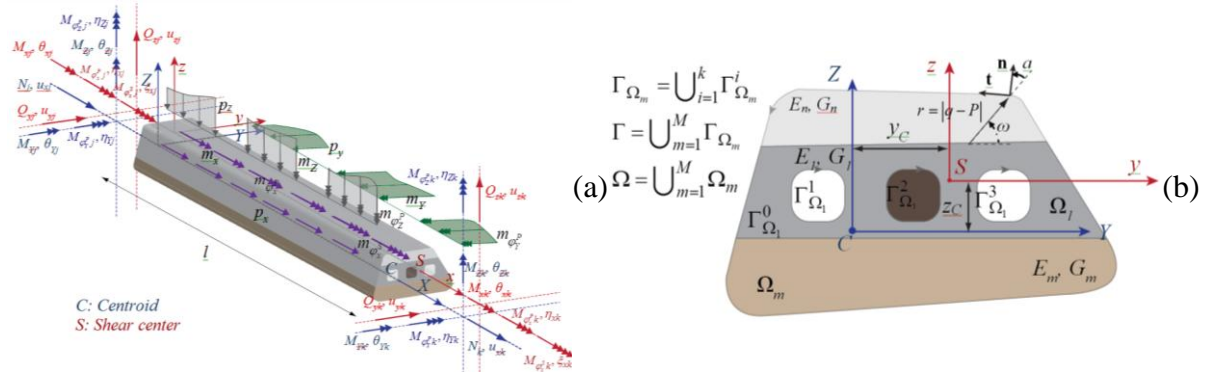


Fig. 1: Prismatic beam element (a) with a composite cross section of arbitrary shape occupying the two dimensional region  $\Omega$  (b).

Within the above described context, in order to take into account nonuniform flexural and torsional warping (including shear lag effect due to both flexure and torsion), in the study of the aforementioned element in each node at the element ends, four additional degrees of freedom are added to the well-known six DOFs of the classical three-dimensional frame element. The additional DOFs include four independent parameters, namely  $\eta_x, \eta_y, \eta_z, \xi_x$  multiplying a shear warping function in each direction ( $\eta_y, \eta_z$ ) and two torsional warping functions ( $\eta_x, \xi_x$ ), respectively. These DOFs describe the “intensities” of the corresponding cross sectional warpings along the beam length, while these warpings are defined by the corresponding warping function ( $\varphi_y^P, \varphi_z^P, \varphi_x^P, \varphi_x^S$ ), depending only on the cross sectional configuration. The corresponding stress resultants of the aforementioned additional DOFs are the warping moments  $M_{\varphi_y^P}, M_{\varphi_z^P}, M_{\varphi_x^P}, M_{\varphi_x^S}$  (bimoments), arising from corresponding normal stress distributions. By this modification the developed element is enhanced with the capability of taking into account shear deformation and shear lag effects due to both flexure and torsion. Thus, the generalized local nodal displacement and nodal load vectors can be written as

$$\{D^i\} = \left[ \begin{array}{cccccccccccc} u_x^{ij} & u_y^{ij} & u_z^{ij} & \theta_x^{ij} & \theta_y^{ij} & \theta_z^{ij} & \eta_x^{ij} & \eta_y^{ij} & \eta_z^{ij} & \xi_x^{ij} & u_x^{ik} & u_y^{ik} & u_z^{ik} & \theta_x^{ik} \\ \theta_y^{ik} & \theta_z^{ik} & \eta_x^{ik} & \eta_y^{ik} & \eta_z^{ik} & \xi_x^{ik} & & & & & & & & & \end{array} \right]^T \quad (1a)$$

$$\{F^i\} = \left[ \begin{array}{cccccccccccc} N^{ij} & Q_y^{ij} & Q_z^{ij} & M_x^{ij} & M_y^{ij} & M_z^{ij} & M_{\varphi_y^P}^{ij} & M_{\varphi_y^S}^{ij} & M_{\varphi_z^P}^{ij} & M_{\varphi_z^S}^{ij} & N^{ik} \\ Q_y^{ik} & Q_z^{ik} & M_x^{ik} & M_y^{ik} & M_z^{ik} & M_{\varphi_y^P}^{ik} & M_{\varphi_y^S}^{ik} & M_{\varphi_z^P}^{ik} & M_{\varphi_z^S}^{ik} & & & & & & \end{array} \right]^T \quad (1b)$$

In eqn. (1a)  $u_x, u_y, u_z, \theta_x, \theta_y, \theta_z$  describe the displacement and rotation components, while  $\eta_x, \xi_x, \eta_y, \eta_z$  are the aforementioned independent warping parameters describing the nonuniform distribution of primary and secondary torsional and primary shear warping, respectively. Index  $i$  denotes the  $i$ -th beam element, while indices  $j, k$  refer to each element end. In eqn. (1b)  $N, Q_y, Q_z, M_x$  are the axial force  $N = EAu_{x,x}$ , shear forces  $Q_i = Q_i^P + Q_i^S$  ( $i = y, z$ ) and twisting moment  $M_x = M_x^P + M_x^S + M_x^T$ , respectively at the element ends.  $Q_i^j$  ( $i = y, z, j = P, S$ ) are the primary and secondary parts of shear forces, while  $M_x^j$  ( $j = P, S, T$ ) are the primary, secondary and tertiary parts of total twisting moment arising from the corresponding shear stress components presented in detail in [1].  $M_{\varphi_x^p}, M_{\varphi_y^p}, M_{\varphi_z^p}, M_{\varphi_x^s}$  are the warping moments due to independent warping parameters  $\eta_x, \eta_y, \eta_z, \xi_x$ , respectively, given as [1]

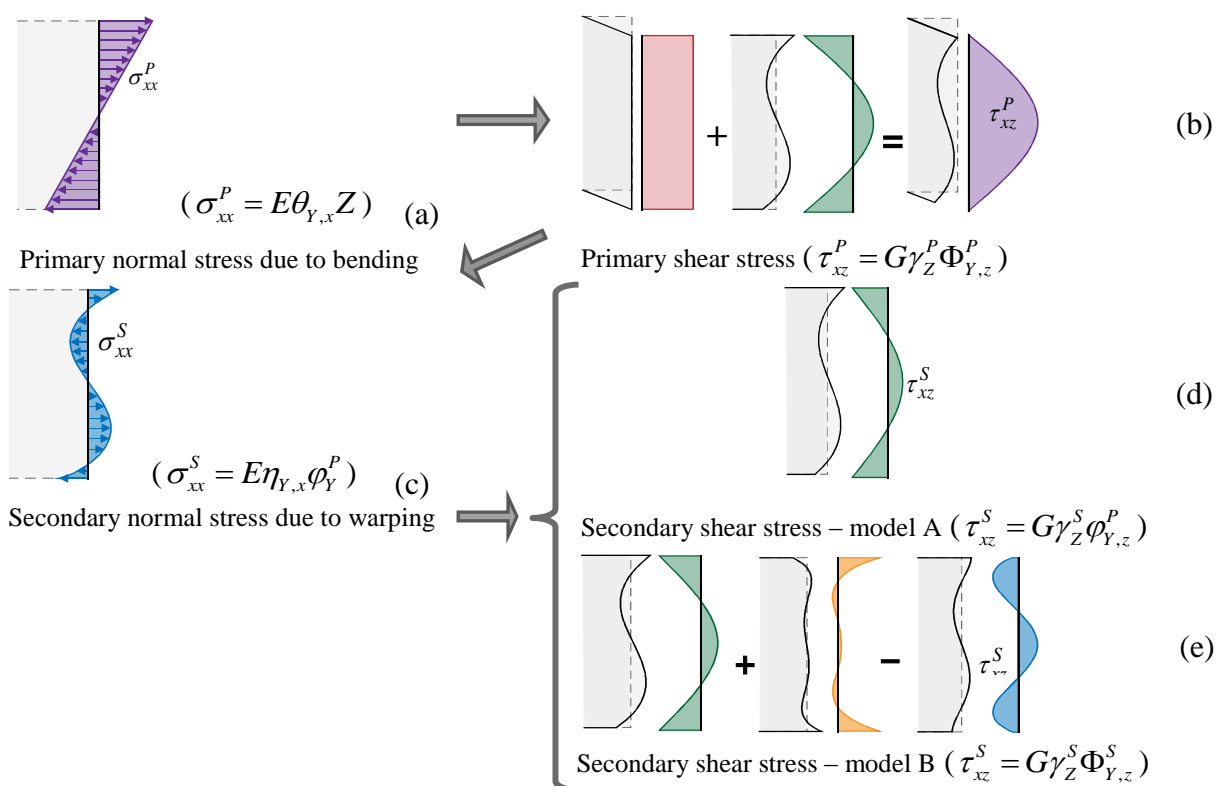


Fig. 2: Sequence of stress generation along the height of a rectangular cross section of a beam under flexure.

$$M_{\varphi_x^p} = E \left( I_{\varphi_x^p \varphi_x^p} \eta_{x,x} + I_{\varphi_y^p \varphi_x^p} \eta_{y,x} + I_{\varphi_z^p \varphi_x^p} \eta_{z,x} \right) \quad M_{\varphi_x^s} = E \left( I_{\varphi_x^s \varphi_x^s} \xi_{x,x} + I_{\varphi_y^p \varphi_x^s} \eta_{y,x} + I_{\varphi_z^p \varphi_x^s} \eta_{z,x} \right) \quad (2a,b)$$

$$M_{\varphi_y^p} = E \left( I_{\varphi_y^p \varphi_y^p} \eta_{y,x} + I_{\varphi_x^p \varphi_y^p} \eta_{x,x} + I_{\varphi_z^p \varphi_y^p} \xi_{x,x} \right) \quad M_{\varphi_z^p} = E \left( I_{\varphi_z^p \varphi_z^p} \eta_{z,x} + I_{\varphi_x^p \varphi_z^p} \eta_{x,x} + I_{\varphi_y^p \varphi_z^p} \xi_{x,x} \right) \quad (2c,d)$$

where  $(\cdot)_{,i}$  denotes differentiation with respect to  $i$  and  $I_{ij}$  ( $i, j = \varphi_x^P, \varphi_x^S, \varphi_y^P, \varphi_z^P$ ) are warping constants given in [1,2].  $\varphi_y^P, \varphi_z^P, \varphi_x^P, \varphi_x^S$  indices denote the aforementioned primary shear and primary and secondary torsional warping functions [1].

The nodal displacement and load vectors given in eqns. (1) are related with a 20x20 local stiffness matrix  $[k^i]$  the coefficients  $k_{jk}^i$  ( $j, k = 1, 2, \dots, 20$ ) of which are obtained by

solving a system of differential equations with respect to  $u_x, u_y, u_z, \theta_x, \theta_y, \theta_z, \eta_x, \eta_y, \eta_z, \xi_x$  formulated as presented in [1], subjected to the corresponding boundary conditions given as

$$a_1 u_x + \alpha_2 N = \alpha_3 \quad \beta_1 u_y + \beta_2 Q_y = \beta_3 \quad \gamma_1 u_z + \gamma_2 Q_z = \gamma_3 \quad \bar{\beta}_1 \theta_z + \bar{\beta}_2 M_z = \bar{\beta}_3 \quad (3a,b,c,d)$$

$$\bar{\gamma}_1 \theta_y + \bar{\gamma}_2 M_y = \bar{\gamma}_3 \quad \tilde{\beta}_1 \eta_z + \tilde{\beta}_2 M_{\varphi_z^p} = \tilde{\beta}_3 \quad \tilde{\gamma}_1 \eta_y + \tilde{\gamma}_2 M_{\varphi_y^p} = \tilde{\gamma}_3 \quad \delta_1 \theta_x + \delta_2 M_x = \delta_3 \quad (3e,f,g,h)$$

$$\bar{\delta}_1 \eta_x + \bar{\delta}_2 M_{\varphi_x^p} = \bar{\delta}_3 \quad \tilde{\delta}_1 \xi_x + \tilde{\delta}_2 M_{\varphi_x^s} = \tilde{\delta}_3 \quad (3i,j)$$

by setting the external loading equal to zero and applying appropriate values to functions  $\alpha_i, \beta_i, \bar{\beta}_i, \tilde{\beta}_i, \gamma_i, \bar{\gamma}_i, \tilde{\gamma}_i, \delta_i, \bar{\delta}_i, \tilde{\delta}_i$  ( $i=1,2,3$ ). According to the nodal load vector, assuming that the span of the beam is subjected to arbitrary loading as described above, the evaluation of  $\{F^i\}$  is accomplished by solving again the aforementioned differential equations [1] for  $\alpha_1 = \beta_1 = \bar{\beta}_1 = \tilde{\beta}_1 = \gamma_1 = \bar{\gamma}_1 = \tilde{\gamma}_1 = \delta_1 = \bar{\delta}_1 = \tilde{\delta}_1 = 1$ ,  $\alpha_2 = \alpha_3 = \beta_2 = \beta_3 = \bar{\beta}_2 = \bar{\beta}_3 = \tilde{\beta}_2 = \tilde{\beta}_3 = \gamma_2 = \bar{\gamma}_2 = \tilde{\gamma}_2 = \tilde{\gamma}_3 = \delta_2 = \delta_3 = \bar{\delta}_2 = \bar{\delta}_3 = \tilde{\delta}_2 = \tilde{\delta}_3 = 0$  at  $x=0, l$ .

As far as the numerical solution is concerned, the formulation of the advanced 20x20 stiffness matrix and corresponding nodal load vector reduces in establishing the components  $u_x, u_y, u_z, \theta_x, \theta_y, \theta_z, \eta_x, \eta_y, \eta_z, \xi_x$  having continuous derivatives up to the second order with respect to  $x$  at the interval  $(0, l)$  and up to the first order at  $x=0, l$ , satisfying the boundary value problem described in [1]. This problem is solved using the Analog Equation Method (AEM), a BEM based method. Application of the boundary element technique yields a system of linear coupled algebraic equations which can be solved without any difficulty. The geometric constants of the cross section [1,2] are evaluated employing a pure BEM approach, i.e. only boundary discretization of the cross section is used.

#### 4. APPLICATION

A curved composite bridge deck (Fig.3a), clamped at its end points  $A, E$  and inhibiting deflection at points  $B, D$ , having a cross section consisting of a concrete ( $E_1 \equiv E_{\text{ref}} = 3.0 \times 10^7 \text{ kPa}, \nu = 0.2$ ) plate stiffened by a steel beam ( $E_2 = 2.1 \times 10^8 \text{ kPa}, \nu = 0.2$ ), forming a box-shaped section (Fig.3b), subjected to a vertical load  $P_z = -600 \text{ kN}$  at point C (Fig.3a) is studied. In Fig.4 deflection  $u_z$  along the composite bridge deck as obtained employing 20x20 stiffness matrix employing either uncorrected stress field (model A) or corrected stress field (model B) is presented as compared with those obtained employing, 14x14 [19], as well as classic 12x12 [19] stiffness matrix. From the obtained results, the significant influence of transverse shear deformation can be verified (classic 12x12 stiffness matrix exhibits significant discrepancies). In Fig.5  $M_Y, M_{\varphi_x^p}, M_{\varphi_y^p}, M_{\varphi_x^s}$  diagrams are presented and in Fig.6 the distribution of  $\sigma_{xx}$  along the boundary of the cross section at  $\bar{x} = 40 \text{ m}$  is presented as compared to the one predicted by engineering beam theory (12x12 stiffness matrix). The discrepancy of maximum normal stress as compared to classical 12x12 stiffness matrix necessitates the inclusion of the additional degrees of freedom, in beam elements.

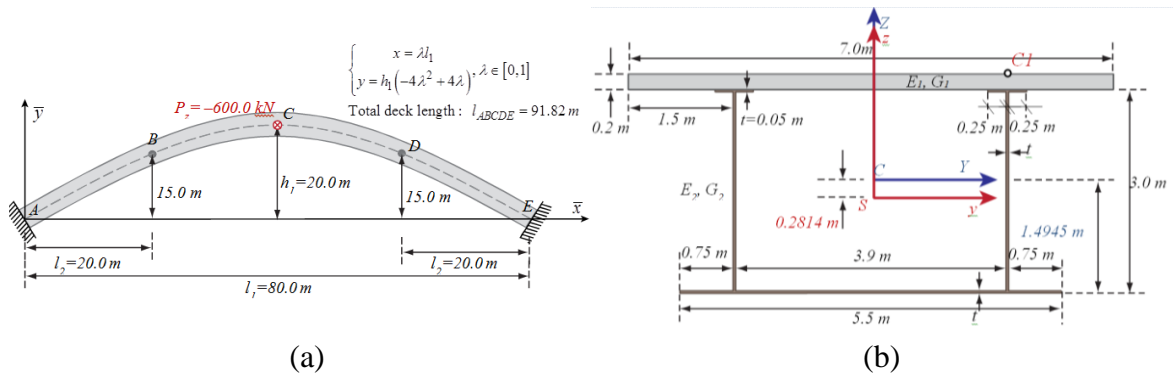


Fig. 3: Plan view (a) and composite cross section (b) of curved bridge deck.

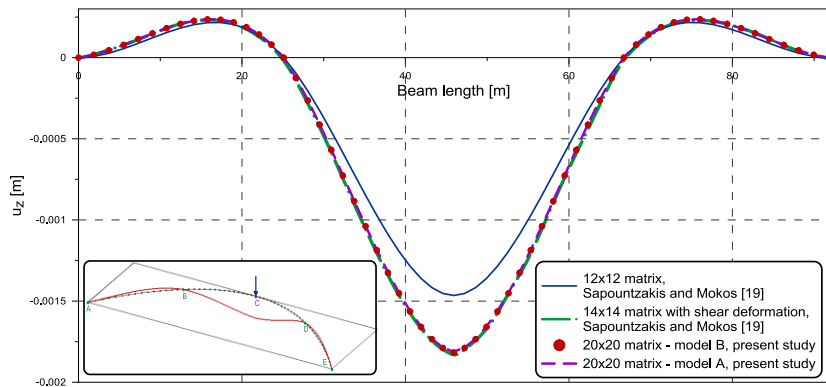


Fig. 4: Deflection  $u_z$  of bridge deck.

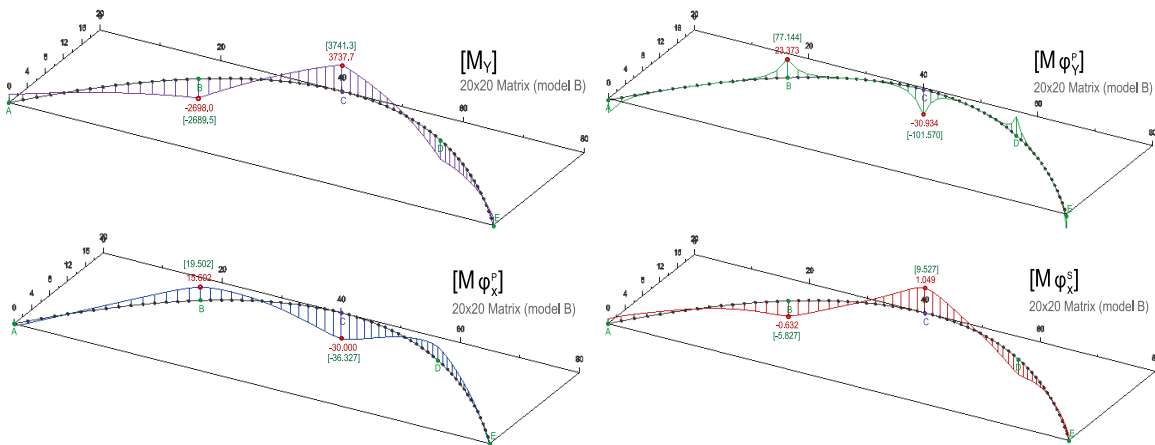
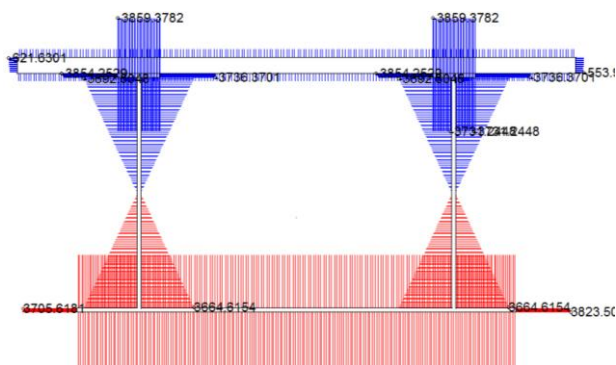
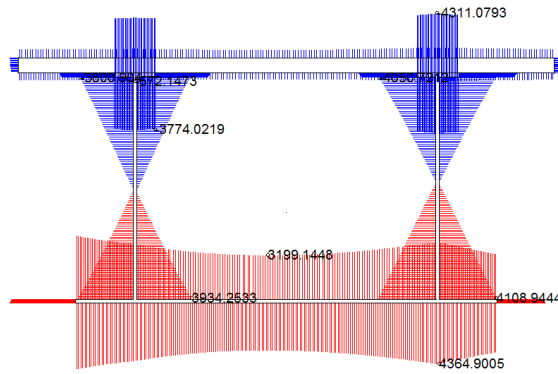


Fig. 5:  $M_Y, M_{\phi_y^p}, M_{\phi_x^p}, M_{\phi_x^s}$  diagrams of bridge deck employing corrected shear stresses (model B). Values in brackets have been obtained employing uncorrected shear stresses (model A).



12x12 matrix:  
 $(\sigma_{xx})_{\max} = 3.8286E+03 \text{ kPa}$   
 (a)



$$20 \times 20 \text{ matrix - model B:}$$

$$(\sigma_{xx})_{\max} = 4.3775\text{E} + 03 \text{ kPa}$$

(b)

Fig. 10. Distribution of  $\sigma_{xx}$  over the boundary of the cross section of beam structure of example 4 at  $\bar{x} = 40$  according to classic  $12 \times 12$  stiffness matrix (a) and  $20 \times 20$  stiffness matrix – model B (b).

## 5. ACKNOWLEDGEMENTS

This research has been co-financed by the European Union (European Social Fund - ESF) and Greek national funds through the Operational Program “Education and Lifelong Learning” of the National Strategic Reference Framework (NSRF) - Research Funding Program: THALES: Reinforcement of the interdisciplinary and/or inter-institutional research and innovation.

## 6. REFERENCES

- [1] I.C. Dikaros and E.J. Sapountzakis, Generalized Warping Analysis of Composite Beams of Arbitrary Cross Section by BEM Part I: Theoretical Considerations and Numerical Implementation. *Journal of Engineering Mechanics ASCE*, in press, DOI: 10.1061/(ASCE)EM.1943-7889.0000775.
- [2] I.C. Dikaros and E.J. Sapountzakis, Generalized Warping Analysis of Composite Beams of Arbitrary Cross Section by BEM Part II: Numerical Applications. *Journal of Engineering Mechanics ASCE*, in press, DOI: 10.1061/(ASCE)EM.1943-7889.0000776.
- [3] V.G. Mokos and E.J. Sapountzakis, Secondary Torsional Moment Deformation Effect by BEM, *International Journal of Mechanical Sciences*, 53 (2011), 897-909.
- [4] V.J. Tsipiras and E.J. Sapountzakis, Secondary Torsional Moment Deformation Effect in Inelastic Nonuniform Torsion of Bars of Doubly Symmetric Cross Section by BEM, *International Journal of Non-linear Mechanics*, 47 (2012), 68-84.
- [5] J.T. Katsikadelis, The Analog Equation Method. A Boundary – only Integral Equation Method for Nonlinear Static and Dynamic Problems in General Bodies, *Theoretical and Applied Mechanics*, 27 (2002), 13-38.
- [6] Sapountzakis E.J. and Mokos V.G. 3-D beam element of composite cross section including warping and shear deformation effects, *Computers and Structures* 2007; **85**:102–116.

## **ΧΩΡΙΚΟ ΣΤΟΙΧΕΙΟ ΔΟΚΟΥ ΓΙΑ ΠΡΟΧΩΡΗΜΕΝΗ ΑΝΑΛΥΣΗ ΚΑΤΑΣΚΕΥΩΝ ΑΠΟ ΧΑΛΥΒΑ**

**Ευάγγελος Ι. Σαπουντζάκης**

Καθηγητής

Σχολή Πολιτικών Μηχανικών, Εθνικό Μετσόβιο Πολυτεχνείο

Πολυτεχνειούπολη Ζωγράφου, Αθήνα 15780

e-mail: [cvsapoun@central.ntua.gr](mailto:cvsapoun@central.ntua.gr)

**Ιωάννης Χ. Δίκαιος**

Πολιτικός Μηχανικός, MSc, Υποψήφιος Διδάκτωρ

Σχολή Πολιτικών Μηχανικών, Εθνικό Μετσόβιο Πολυτεχνείο

Πολυτεχνειούπολη Ζωγράφου, Αθήνα 15780

e-mail: [dikarosgiannis@gmail.com](mailto:dikarosgiannis@gmail.com)

### **1. ΠΕΡΙΛΗΨΗ**

Στην παρούσα εργασία, παρουσιάζεται η μεθοδολογία για τη μόρφωση ενός διευρυμένου «20x20» μητρώου στιβαρότητας και του αντίστοιχου μητρώου επικόμβιας φόρτισης χωρικού στοιχείου δοκού τυχούσας σύμικτης διατομής (η περίπτωση τυχούσας ομογενούς διατομής αντιμετωπίζεται ως ειδική περίπτωση) λαμβάνοντας υπόψη τη γενικευμένη επιρροή της ανομοιόμορφης στρέβλωσης (διατμητική υστέρηση από κάμψη και στρέψη). Η ανομοιόμορφη κατανομή των στρεβλώσεων που ευθύνεται για το φαινόμενο της διατμητικής υστέρησης λαμβάνεται υπόψη χρησιμοποιώντας τέσσερις ανεξάρτητες παραμέτρους στρέβλωσης, οι οποίες πολλαπλασιάζουν δύο συναρτήσεις διατμητικής στρέβλωσης (μία σε κάθε διεύθυνση) και δύο συναρτήσεις στρεπτικής στρέβλωσης, αντίστοιχα, που προσδιορίζονται λύνοντας αντίστοιχα προβλήματα συνοριακών τιμών. Δέκα προβλήματα συνοριακών τιμών ως προς τα κινηματικά μεγέθη διατυπώνονται και λύνονται με χρήση μεθοδολογίας που βασίζεται στη Μέθοδο Συνοριακών Στοιχείων. Αξίζει εδώ να αναφερθεί ότι το πεδίο τάσεων που προκύπτει από το υιοθετούμενο πεδίο μετατοπίσεων οδηγεί σε παραβίαση της τοπικής εξίσωσης ισορροπίας κατά τη διαμήκη έννοια και της αντίστοιχης συνοριακής συνθήκης λόγω της ανακρίβειας που προκύπτει στις διατμητικές τάσεις. Συνεπώς, στην παρούσα εργασία, τα προβλήματα συνοριακών τιμών που επιλύονται διατυπώνονται χρησιμοποιώντας βελτιωμένο πεδίο τάσεων το οποίο προκύπτει με κατάλληλη διόρθωση των συνιστωσών διατμητικής τάσης. Οι συναρτήσεις στρέβλωσης καθώς και οι γεωμετρικές σταθερές, συμπεριλαμβανομένων και των ανώτερων σταθερών λόγω στρέβλωσης, υπολογίζονται με εφαρμογή της αμιγούς Μεθόδου Συνοριακών Στοιχείων (απαιτείται διακριτοποίηση μόνον του συνόρου της διατομής). Μέσω αριθμητικών εφαρμογών καταδεικνύονται οι αποκλίσεις που παρουσιάζουν τα κλασικά στοιχεία δοκού (12x12, 14x14 μητρώα στιβαρότητας) συγκρινόμενα με το παρών εξελιγμένο στοιχείο δοκού.